Supramolecular Chemistry
Publication details, including instructions for authors and subscription information:
http://www.informaworld.com/smpp/title~content=t713649759

Modelling triazolophane-halide binding equilibria using Sivvu analysis of UV-vis titration data recorded under medium binding conditions

Yongjun Li[a]; Douglas A. Vander Griend[b]; Amar H. Flood[a]
[a] Department of Chemistry, Indiana University, Bloomington, USA [b] Department of Chemistry & Biochemistry, Calvin College, Grand Rapids, USA

To cite this Article Li, Yongjun , Griend, Douglas A. Vander and Flood, Amar H.(2009) 'Modelling triazolophane-halide binding equilibria using Sivvu analysis of UV-vis titration data recorded under medium binding conditions', Supramolecular Chemistry, 21: 1, 111 — 117
To link to this Article: DOI: 10.1080/10610270802527051
URL: http://dx.doi.org/10.1080/10610270802527051

Supramolecular Chemistry
Vol. 21, Nos. 1–2, January–March 2009, 111–117

Taylor & Francis
Taylor & Francis Group

Modelling triazolophane–halide binding equilibria using Sivvu analysis of UV–vis titration data recorded under medium binding conditions

Yongjun Li[a], Douglas A. Vander Griend[b1] and Amar H. Flood[a]*

[a]*Department of Chemistry, Indiana University, Bloomington, USA;* [b]*Department of Chemistry & Biochemistry, Calvin College, Grand Rapids, USA*

(*Received 12 July 2008; final version received 3 October 2008*)

Two different models that calculate association constants from UV–vis titration data have been evaluated for the 1:1 binding between triazolophane receptor ([Host] = 1–13 μM) and various halides F^-, Cl^-, Br^- and I^- in CH_2Cl_2 ($K_a \approx 10^3$–10^6 M^{-1}). The Drago model fits the ΔA values at a single wavelength as a function of the added guest concentration. The new computer program Sivvu performs equilibrium-restricted factor analysis using all the wavelengths of the dataset simultaneously. Both models generate comparable K_a values, and both provide a means to assess the accuracy of the binding constant determination: K_a [host] < 12. Analysis with Sivvu (1) allows the number of unique chemical absorbers to be identified in an unbiased manner. This analysis allowed for a 2:1, triazolophane:F^- intermediate to be identified and included in the model. Sivvu also (2) allows alternate models to be quickly evaluated, (3) generates more accurate binding constants, and (4) generates the extinction profiles for each absorbing species in solution.

Keywords: anion receptor; CH hydrogen bonding; host–guest chemistry; spectrophotometric titration; triazolophane

Introduction

Accurate determination of the binding affinity between a host and its guest (Equation (1)) is the first step towards an understanding of their supramolecular chemistry (*1*). When the thermodynamic evaluation is extended to ΔH and ΔS, the supramolecular effects can begin (*2*) to be understood at deeper levels (*3*). This information serves as the basis for both understanding and applications in diverse areas such as biochemistry (*4*), sensing (*5*), molecular transport (*6*) and template-directed synthesis (*7*). Before thermodynamic values can be interpreted in these contexts (*8*), several issues relating to the primary data must be resolved: (1) the identification of the binding stoichiometry, typically achieved using a Job's Plot analysis (*9*); (2) the utilisation of an appropriate chemical model for the host–guest system (*10*); and (3) the evaluation of the appropriateness of the titration experiment for determining the thermodynamic values accurately (*9*, *11*)

$$\text{Host} + \text{Guest} \rightleftharpoons \text{Host–Guest}, \tag{1}$$

$$K_a = \frac{[\text{Host–Guest}]_e}{[\text{Host}]_e[\text{Guest}]_e}. \tag{2}$$

Several different kinds of measurements can be used to track changes in the solution composition throughout a titration. NMR spectroscopy provides a rich amount of structural information. NMR is good for moderate binding strengths ($K_a = 1$–10^3 M^{-1}), but requires relatively high concentrations and does not monitor the equilibrium concentrations directly unless the host–guest complex is undergoing slow exchange on the NMR timescale. Isothermal titration microcalorimetry (ITC) can provide an accurate thermodynamic profile (ΔG, ΔH, ΔS and ΔC_p) of the entire system. These profiles are superior to van't Hoff plots, which are heavily correlated on account of the fact that the ΔH and ΔS stemming from them are obtained from the same set of data. ITC can also provide information about the stoichiometry. A primary drawback stems from the sensitivity of ITC to heat absorbing or evolving equilibria which are not involved with the host–guest interaction. This issue is compounded by the absence of direct structural data to corroborate the proposed model (*1b*) and, therefore, often relies upon appropriate control studies. Spectrophotometric measurements are complementary to these methods when characterising host–guest complexation with reasonably large binding constants ($K_a = 10^3$–10^7 M^{-1}).[2] We are benchmarking the software package Sivvu (*12*), which was created specifically for the purpose of fitting UV–vis data to chemical equilibria.

Sivvu is designed to model UV–vis titration data using equilibrium-restricted factor analysis. When the goal is the quantification of thermodynamic equilibria, having the right model is critical. This is facilitated in Sivvu by a purely mathematical treatment of the data, i.e. unrestricted

*Corresponding author. Email: aflood@indiana.edu

ISSN 1061-0278 print/ISSN 1029-0478 online

DOI: 10.1080/10610270802527051
http://www.informaworld.com

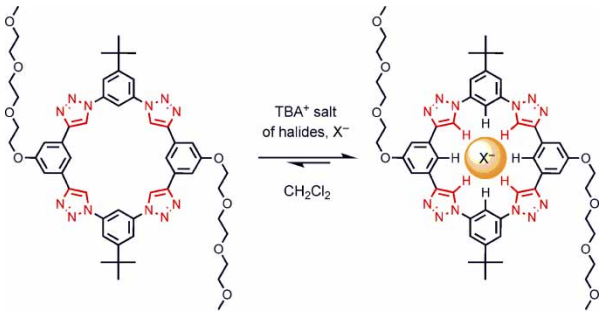

Scheme 1. Schematic representation of **T** encapsulating halides by means of CH hydrogen bonding.

by a model of the host–guest chemistry, and therefore provides an unbiased specification of the number of absorbing components present. Consequently, the model of the host–guest chemistry can be constructed to accommodate the appropriate number of absorbers. On the basis of the model, extinction profiles of each absorbing species are generated. This method of analysis then refines the K_a values associated with each equilibrium present in the model as a means to account for the titration data, i.e. the model confines and restricts the scope of the analysis. This methodology enables the user to determine the model that best conforms to all the observations. All of these features were employed in the seminal paper addressing the sequential binding of 2,2′-bipyridine to the solvated Ni^{2+} cation, including the application of the data to a subsequent kinetics analysis of ligand exchange (*12*). In the present communication, we describe the use of Sivvu to investigate the halide binding (*13*) to triazolophane (**T**) (*14*, *15*) (Scheme 1).

The precautions and qualifications for titration and modelling are equally valid regardless of the technique used to measure the titration data. The titration experiment requires the quality control extolled in general chemistry laboratories with acid-base titrations, including accurate mass and volume measurements. Additionally, volume corrections and strictly constant temperature are worthwhile when aiming to thermodynamically model data. On account of the nonlinear relationship between binding constants and equilibrium concentrations, which are proportional to absorbance, the titration experiment must be carried out at suitable concentrations in order to evaluate the K_a (Equation (2)) accurately. Specifically, there must be sufficient guest added to generate an appreciable amount of the host–guest complex while retaining weak-binding conditions (*11*). This ensures that the equilibrium concentrations of all species in solution, $[Host]_e$, $[Guest]_e$ and $[Host–Guest]_e$, will be sensitive to the binding constant and vice versa. We have distilled the meaning of these guidelines for 1:1 binding as follows. Firstly, for a system to be in a weak or medium binding regime, the mathematical product of K_a and the total host concentration used for the titration should be equal to or less than 12, i.e. $K_a[Host] < 12$. This limit implies that at the point in the titration with equimolar amounts of guest and host, the degree of complexation should be less than 75%. Secondly, enough of the guest must be added in order to progress the degree of complexation from at least 20%, and through to and beyond 80% completion during the entire titration. While these criteria are not intended to be strict rules, they do provide straightforward guidance for the selection of relative concentrations to use in UV–vis titration experiments for 1:1 binding.

We have selected the 1:1 binding between a **T** reported previously (*13*) to verify that Sivvu reproduces the binding affinities obtained from traditional single-wavelength modelling using the Drago method (*10*) and to investigate the impact of these quality control factors on the binding constants. Our results using Sivvu reveal the stepwise 2:1 then 1:1 binding with F^- that was not detected using traditional methods.

Methods

Unrestricted factor analysis to determine the number of absorbing species

Factor analysis (*16*) can be defined as a mathematical technique for determining what fraction of a set of data curves can be reconstructed as a linear combination of a small and arbitrary number of fundamental curves. If every curve in the dataset is a multiple of the same fundamental curve, then the entire set can be reconstructed from that single curve, and there is only one principle factor in the data. If a series of curves all intersect at an isosbestic point, this indicates visually that there are just two distinct fundamental curves. For any given dataset, more than two fundamental curves may be necessary, but the key question is how many are necessary to account for all the signal information, rather than noise, in the dataset. An additional curve will always increase the fraction of data accounted for, however, after a certain number of curves, the rate of improvement levels out because it is only accounting for random noise in the data.

This unrestricted factor analysis, i.e. unrestricted by any chemical model, provides an unbiased specification of the number of absorbing components present in UV–vis data. No restrictions are placed on the shapes of the curves or relationships between them. There are therefore many possible sets of fundamental curves for a given dataset, but all will consist of the same number of fundamentals. Such a purely mathematical treatment of the data will produce factors that fall off in significance. The first factor will be a fundamental, which by itself can be used to reconstruct the greatest fraction of the dataset. The second will then be that factor that can account for the greatest fraction of the dataset that the first did not. Once all the signal

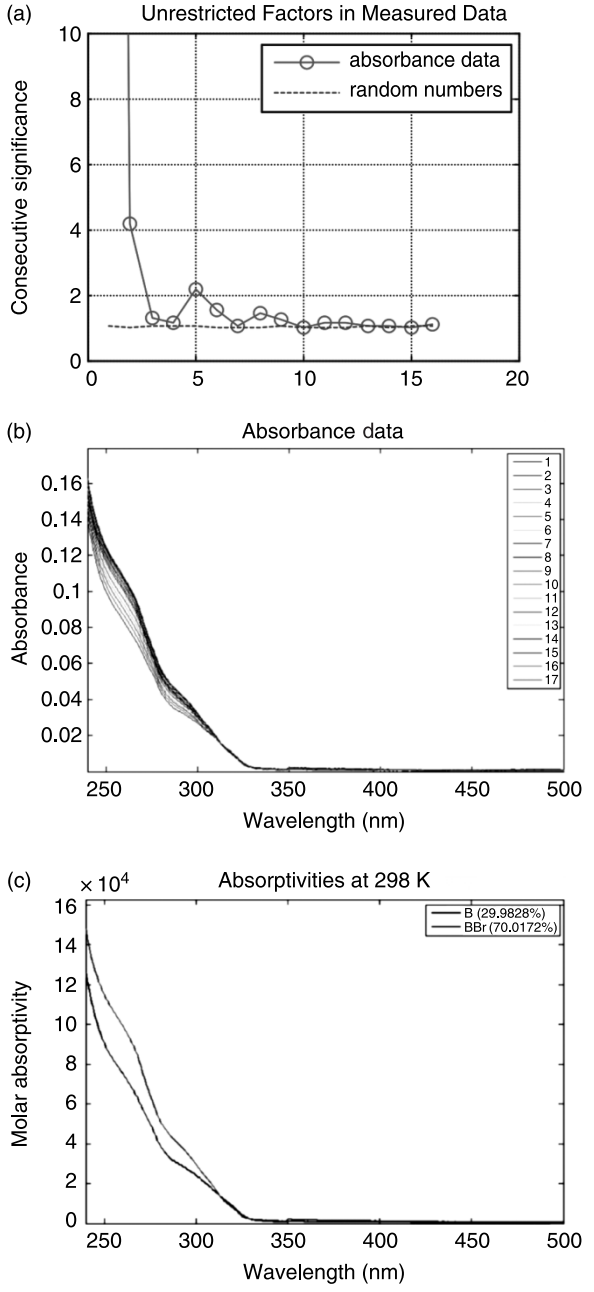

Figure 1. Representative screen shots from Sivvu of the (a) unrestricted factor analysis for the (b) titration of **T** with TBABr and (c) the resulting extinction spectra.

information in the dataset is accounted for, additional factors accounting for random noise will fall in significance at a very characteristic rate of about 10%. An unrestricted factor analysis for the titration (Figure 1(a)) of TBABr into a solution of the **T** shows (Figure 1(b)) that the first factor is more than 10 times more significant than the second factor, which itself is ~4 times more significant than the third. The relative significance of the third factor is typical of random noise. Therefore, two absorbing factors are required to account for the titration data.

Restricted factor analysis to determine the association constants

The chemical model that accounts for all of the absorbing species will then be used to restrict the factor analysis. In this manner each of the absorbing factors will conform to the relationships of chemical equilibria, and the molar absorptivity values will all be positive. With these restrictions, there should be only one viable answer that still accounts for all of the signal information in the entire dataset. For the titration with TBABr, the model shown in Equation (1) was used to fit the data to obtain the extinction spectra (Figure 1(c)). More worked examples of Sivvu are included in the Supporting Information (available online).

Results and discussion

T is a UV-absorbing compound with a series of indistinct shoulders. The spectra (Figure 2) display little change in shape and a modest increase in intensity upon halide binding. Before any modelling of the data, Sivvu can be used to confirm the stoichiometry of the binding event. The break down of the mathematically significant factors (Table 1) that exist in the set of curves that comprise each of the seven datasets was conducted using an unrestricted analysis of the entire dataset. The analysis confirms that in most cases there are only two species in solution which absorb over this range. There are two exceptions. In the case of iodide, which is the only halide that itself absorbs above 240 nm, it is identified as a third factor that is eight times more significant than the fourth factor (Supporting Information). Regardless, this result is consistent with the 1:1 binding model. What was unexpected was the third factor observed during the F^- titration which is seven times more significant than the fourth factor (Supporting Information). On account of the fact that F^- does not absorb, we assigned this to a 2:1 complex. This additional equilibrium is included in the model chemistry from which one obtains a K_1 and K_2 (Equations (3) and (4)). The observed stepwise 2:1 then 1:1 binding (Supporting Information) has been seen to differing degrees in four other anion-receptor complexes (*17–20*). The unrestricted factor analysis of Sivvu obviates the need to perform a separate Job's Plot analysis.

$$\mathbf{T} + F^- \rightleftharpoons \mathbf{T}{\cdot}F^- (K_1), \quad (3)$$

$$\mathbf{T}{\cdot}F^- + \mathbf{T} \rightleftharpoons \mathbf{T}_2{\cdot}F^- (K_2). \quad (4)$$

The association constants (Table 2) for the binding between **T** and the tetrabutylammonium (TBA^+) salts of F^-, Br^- and I^- in CH_2Cl_2, as well as those of TBACl using various host concentrations, have been determined. Both a single-wavelength analysis (*10*, *13*) (265 or 315 nm) and a multi-wavelength analysis (240–500 nm) with Sivvu have been conducted. The incomplete 1:1 binding model for

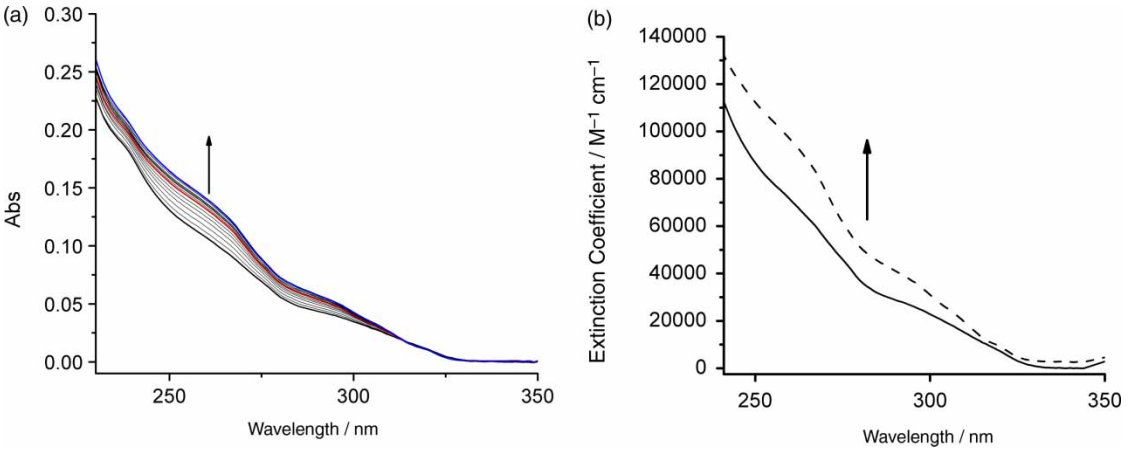

Figure 2. (a) UV–vis titration data of TBACl into 1.5 μM of **T** (CH_2Cl_2, 298 K) highlighting the spectra after 1.0 (red) and 8.3 (blue) equivalents, and (b) UV–vis molar extinction spectra calculated using Sivvu for the uncomplexed **T** (solid line) and the bound state with Cl^- (dashed line).

Table 1. Unrestricted weight of the mathematical factors that additively comprise the curves of each dataset[a].

Factors	F^- 13 μM (%)	Br^- 1.1 μM	I^- 12 μM (%)	Cl^- 12 μM (%)	Cl^- 6 μM (%)	Cl^- 3 μM (%)	Cl^- 1.5 μM (%)
1	97.7	97.5	87.3	97.8	92.0	97.7	97.2
2	1.5	1.3	11.4	1.8	1.7	1.7	1.6
3	0.5	0.3	0.9	0.1	0.1	0.2	0.3
4	0.1	0.2	0.1	0.1	0.1	0.1	0.3
5	0.0	0.2	0.0	0.0	0.1	0.1	0.2

[a] Wavelength range is 240–500 nm, except for I^-, in which case it is 270–500 nm.

Table 2. Association constants and the parameters related to the accuracy assessments for halide binding to **T** (CH_2Cl_2, 298 K) based on a UV–vis titration.

Halide	$[H]_{total}$ (mM)	K_a(Drago)[a] (M^{-1})	K_a(Sivvu)[b,c] (M^{-1})	$[H]_{total}{\cdot}K_a$ (Drago/Sivvu)	Complexation[d] (Drago (%)/Sivvu (%))
F^-	13	230,000 ± 20,000	154,500 ± 1,900 K_1 = 626,000 ± 3,400 K_2 = 55,000 ± 4,300	3.0/2.0	57/50
Br^-	1.1	4,200,000 ± 300,000	3,518,400 ± 2,800	4.6/3.9	63/60
I^-	12	19,000 ± 2,000	5,800 ± 40	0.23/0.07	16/6
Cl^-	12	1,600,000 ± 400,000	2,388,000 ± 14,000	19/29	80/83
Cl^-	6	2,500,000 ± 500,000	2,659,000 ± 26,000	15/16	77/78
Cl^-	3	4,700,000 ± 700,000	4,416,000 ± 19,000	14/13	77/76
Cl^-	1.5	5,100,000 ± 400,000	4,555,000 ± 15,000	7.7/6.8	70/68

[a] Based in a 1:1 model and fitting the data to the Drago model

$$\Delta A = \varepsilon_{complex} \times \{([Host]_i + [X^-] + (1/K_a)) - \{([Host]_i + [X^-] + (1/K_a))^2 - (4 \times [Host]_i \times [X^-])\}^{1/2}\}/2.$$

[b] The Sivvu analyses are was based on the 240–500 nm region for F^-, Cl^- and Br^- and for the 270–500 nm region for I^- with I^- itself included as a third absorber.
[c] The 1:1 binding model for F^- is included solely for the purposes of comparison to the 1:1 Drago model. Stepwise 2:1 (K_2) then 1:1 (K_1) binding fits are also included.
[d] The degree of complexation for an equimolar host/guest solution.

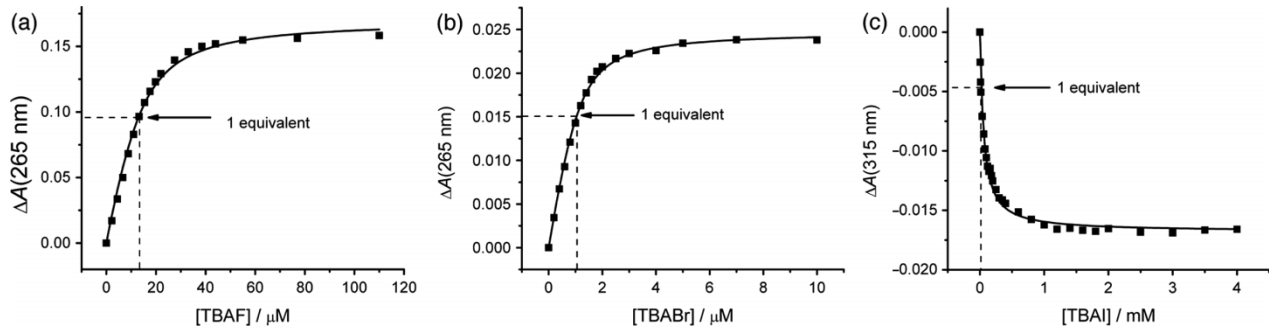

Figure 3. UV–vis titration absorbance profiles and the fit of the data to the 1:1 Drago model for binding of **T** (CH_2Cl_2) with (a) TBAF ([**T**] = 13 μM), (b) TBABr ([**T**] = 1.1 μM), (c) TBAI ([**T**] = 12 μM). The arrows indicate 1:1 host:guest molar ratios.

F^- was included for the purposes of comparison between the Drago method and Sivvu. In order to assess any size effects associated with the halides, the K_1 binding constant for F^- needs to be compared with the K_a values for the other halides. The size selective binding that was observed (*13*) in the order from the strongest to the weakest $Cl^- \sim Br^- > F^- > I^-$, when using only the Drago method, is preserved after analysis with Sivvu and when taking the new model for the F^- binding into account.

The experiments with TBAF, TBABr and TBAI cover the entire range of complexation and are consistent with medium to weak binding (K_a[Host] < 12). The absorbance profiles (Figure 3) for these three halides confirm that they are all less than 75% complexed at the point when 1.0 equivalent of the halide has been added. The Drago and Sivvu methods for 1:1 models are somewhat comparable, but since the latter models the entire dataset rather than just a single wavelength, it results in much smaller errors (~1%). Sivvu calculates error by calculating the deviations that stem from repeatedly optimising models on random subsets of the data, specifically with 10% of the curves and 20% of the wavelengths omitted.

The greatest discrepancy between the two sets of values occurs for the iodide case. This is due in large part to the fact that iodide itself is a significant absorber below 280 nm and Sivvu can take this directly into account, whereas the Drago method cannot. Indeed, at 315 nm, the wavelength used for the Drago method, iodide accounts for over 3% of the absorbance by the end of the titration.

Titrations with TBACl were conducted over a range of **T** concentrations (12, 6, 3 and 1.5 μM) as a means to evaluate our proposed accuracy criteria. The normalised absorbance profiles (Figure 4) for the highest and lowest concentrations were fitted using the Drago method and show that the degree of complexation covers the entire range (0–100%). The binding constants (Table 1) increase monotonically with decreasing host concentration, regardless of which method is used to model the data. The inconsistency in the value of the binding constant is to be expected. When the **T** concentration is 12 μM, the system is under the tight binding conditions (K_a[Host] = 20). When the **T** concentration is eight times less, the system is under medium binding conditions (K_a[Host] = 7.5), and this confers more accuracy on the modelling of the binding constant. This enhanced accuracy can be seen visually from the shift, albeit subtle, in the curvature of the profiles from sharp to shallow (Figure 4). Analysis with Sivvu using the full wavelength range resulted in smaller errors and a tighter upward trend in the K_a values as the system was diluted into the medium-binding regime.

Concentration profiles have been generated (Figure 5) by Sivvu for the titrations with TBACl at [Host] = 12 and 1.5 μM. They provide a similar representation of the degree of complexation as that obtained from the single-wavelength plots (Figure 4), and also provide a means to visually ascertain the degree of binding. These findings confirm that the strength of host–guest binding restricts the applicability of the UV–vis titration method to model binding constants accurately. Consequently, it is important

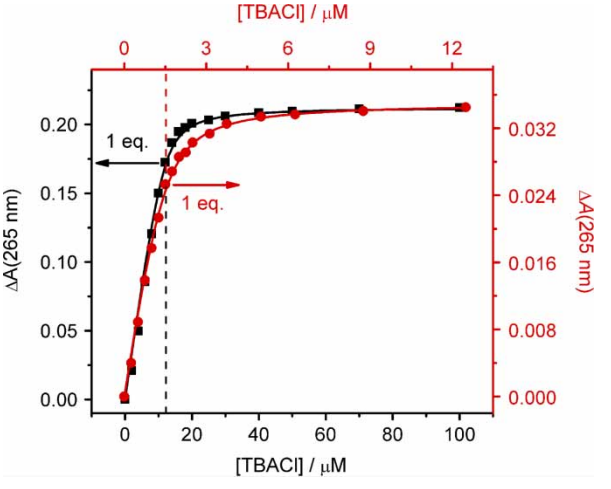

Figure 4. Normalised absorbance profiles for the titration of **T** at different concentrations of TBACl (12 and 1.5 μM, CH_2Cl_2) at 265 nm.

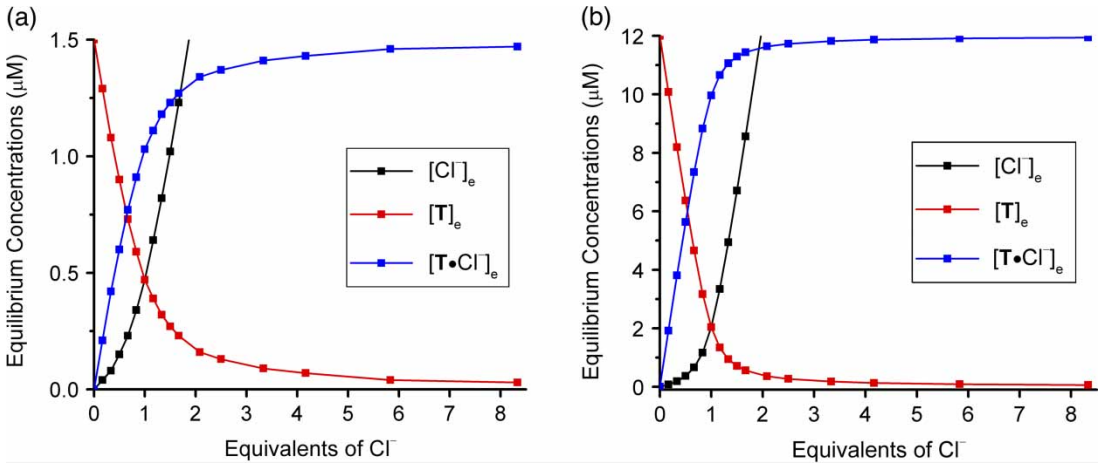

Figure 5. Concentration profiles of **T** at (a) 1.5 μM and (b) 12 μM, with TBACl (CH_2Cl_2, 298 K).

to report the concentration at which the titration was conducted to allow the accuracy of the K_a determinations to be judged.

In addition to using all of the data in the dataset to refine the equilibrium constants much more accurately, Sivvu also calculates the molar extinction coefficient for each absorber at every measured wavelength. These values can then be assimilated into a complete molar extinction profile over the range of interest. The full spectrum for the Cl^- complex (Figure 2) and of the three other **T**–halide complexes have been calculated (Supporting Information). The spectra of $\mathbf{T}\cdot X^-$ ($X^- = F^-$, Cl^-, Br^- and I^-) are similar to each other with intensity increases and a slight intensity decrease at wavelengths longer than 310 nm. These molar extinction profiles are particularly useful when it is difficult or even impossible to isolate particular species in solution either owing to the speed at which they equilibrate or stemming from the presence of overlapping spectra of more dominant solution species.

As a case in point, we have been able to reveal the UV–vis molar absorptivity profile of the 2:1 $\mathbf{T}_2$:F^- dimer complex even though it accounts for only 9.3% of the dataset (Supporting Information). More convincingly, the spectrum of the $\mathbf{T}_2$:F^- system is consistent with a sandwich complex. The molar absorptivity profile can be divided by two in order to normalise the spectrum according to the number of **T**s. Compared with **T** alone, the sandwich complex has decreased intensity across most of the absorbing regions. This **T** is known to aggregate (*13*). The molar absorption spectra of **T** in its aggregated state and also upon dilution from 1 mM down to 1 μM (Supporting Information) show the aggregated species to have a lower overall molar absorptivity across all wavelengths. The similarities upon dimerization in the sandwich complex and aggregation at higher concentrations of the **T** alone are consistent with formation of a sandwich complex.

Conclusions

We have shown how Sivvu can be used in the place of the traditional Drago and Job's Plot methods to model binding equilibria and verify binding stoichiometry obtained from UV–vis titrations. The limits of both models rely upon the initial experimental conditions of the titration such that sufficiently weak binding (K_a[Host] < 12) is achieved. Sivvu uses all available wavelengths to obtain more accurate K_a values and complete molar extinction curves for the complexes. Sivvu provides greater flexibility by accounting for minor absorbing species, as is the case of I^- as well as by identifying minor host–guest species as seen for the 2:1 complex $\mathbf{T}_2\cdot F^-$.

Acknowledgements

DVG would like to thank the Research Corporation and the ACS-PRF for funding.

Notes

1. Email: dvg@calvin.edu
2. We believe that 10^7 M^{-1} binding can be accurately determined under the right experimental conditions, e.g., strong absorptions.

References

(1) (a) Steed, J.W.; Atwood, J.L. *Supramolecular Chemistry*; Wiley-VCH: Weinheim, 2000. (b) Schmidtchen, F.P. In *Analytical Methods in Supramolecular Chemistry*; Schalley, C.A., Ed.; Wiley-VCH: Weinheim, 2007.

(2) Sessler, J.L.; Gross, D.E.; Cho, W.S.; Lynch, V.M.; Schmidtchen, F.P.; Bates, G.W.; Light, M.E.; Gale, P.A. *J. Am. Chem. Soc.* **2006**, *128*, 12281–12288.

(3) (a) Schmidtchen, F.P. *Org. Lett.* **2002**, *4*, 431–434. (b) Moonen, N.N.P.; Flood, A.H.; Fernandez, J.M.; Stoddart, J.F. *Top. Curr. Chem.* **2005**, *262*, 99–123. (c) Schmidtchen, F.P. *Coord. Chem. Rev.* **2006**, *250*, 2918–2928.

(4) (a) Silverman, D.N.; Lindskog, S. *Acc. Chem. Res.* **1988**, *21*, 30–36. (b) Christianson, D.W.; Lipscomb, W.N. *Acc. Chem. Res.* **1989**, *22*, 62–69. (c) Kubik, S.; Reyheller, C.; Stuwe, S. *J. Incl. Phenom.* **2005**, *52*, 137–187.
(5) (a) Badr, I.H.A.; Diaz, M.; Hawthorne, M.F.; Bachas, L.G. *Anal. Chem.* **1999**, *71*, 1371–1377. (b) Mizukami, S.; Nagano, T.; Urano, Y.; Odani, A.; Kikuchi, K. *J. Am. Chem. Soc.* **2002**, *124*, 3920–3925. (c) Martinez-Manez, R.; Sancenon, F. *Chem. Rev.* **2003**, *103*, 4419–4476. (d) Beer, P.D.; Hayes, E.J. *Coord. Chem. Rev.* **2003**, *240*, 167–189.
(6) (a) Sato, T.; Konno, H.; Tanaka, Y.; Kataoka, T.; Nagai, K.; Wasserman, H.H.; Ohkuma, S. *J. Biol. Chem.* **1998**, *273*, 21455–21462. (b) Yamamoto, D.; Kiyozuka, Y.; Uemura, Y.; Yamamoto, C.; Takemoto, H.; Hirata, H.; Tanaka, K.; Hioki, K.; Tsubura, A. *J. Cancer Res. Clin.* **2000**, *126*, 191–197. (c) Dutzler, R.; Campbell, E.B.; Cadene, M.; Chait, B.T.; MacKinnon, R. *Nature* **2002**, *415*, 287–294. (d) Accardi, A.; Miller, C. *Nature* **2004**, *427*, 803–807.
(7) Vickers, M.S.; Beer, P.D. *Chem. Soc. Rev.* **2007**, *36*, 211–225.
(8) Schneider, H.-J.; Yatsimirsky, A. *Principles and Methods in Supramolecular Chemistry*; Wiley-VCH: Weinheim, 2000.
(9) Connors, K.A. *Binding Constants*; Wiley: New York, 1987.
(10) Long, J.R.; Drago, R.S. *J. Chem. Edu.* **1982**, *59*, 1037–1089.
(11) Hirose, K. In *Analytical Methods in Supramolecular Chemistry*; Schalley, C.A., Ed.; Wiley-VCH: Weinheim, 2007.
(12) Vander Griend, D.A.; Bediako, D.K.; DeVries, M. J.; DeJong, N.A.; Heeringa, L.P. *Inorg. Chem.* **2008**, *47*, 656–662.
(13) Li, Y.; Flood, A.H. *J. Am. Chem. Soc.* **2008**, *130*, 12111–12122.
(14) Li, Y.; Flood, A.H. *Angew. Chem., Int. Ed.* **2008**, *47*, 2649–2652.
(15) (a) Chande, M.S.; Athalye, S.S. *Synth. Commun.* **2000**, *30*, 1667–1674. (b) Ray, A.; Manoj, K.; Bhadbhade, M. M.; Mukhopadhyay, R.; Bhattacharjya, A. *Tetrahedron Lett.* **2006**, *47*, 2775-2778. (c) Chande, M.S.; Barve, P.A.; Khanwelkar, R. R.; Athalye, S.S.; Venkataraman, D.S. *Can. J. Chem.* **2007**, *85*, 21–28.
(16) Malinowski, E. R. *Factor Analysis in Chemistry*, 3rd ed.; John Wiley and Sons Inc., New York, 2002.
(17) Hossain, M.A.; Llinares, J.M.; Powell, D.; Bowman-James, K. *Inorg. Chem.* **2001**, *40*, 2936–2937.
(18) (a) Choi, K.H.; Hamilton, A.D. *J. Am. Chem. Soc.* **2001**, *123*, 2456–2457. (b) Choi, K.H.; Hamilton, A.D. *J. Am. Chem. Soc.* **2003**, *125*, 10241–10249.
(19) Kubik, S.; Goddard, R.; Kirchner, R.; Nolting, D.; Seidel, J. *Angew. Chem., Int. Ed.* **2001**, *40*, 2648–2651.
(20) Custelcean, R.; Remy, P.; Bonnesen, P.V.; Jiang, D.E.; Moyer, B.A. *Angew. Chem., Int. Ed.* **2008**, *47*, 1866–1870.